



collection mechanism and a technique on process level to reduce soft errors effects is presented. The doping profiles and devices regions dimensions where analyzed with the data from [3] to create the device proposed in this work. At the next section the developed model is presented.

### 3. MODELED DEVICE

The first step to create a device model is to define a strategy to build the MESH. The MESH is a structure where the device regions are created and their sections and points define where physic calculations are done to evaluate the simulations. If the MESH is defined with too much simulation points will lead to many days of simulation, but if this number is small the results of the simulation will be too far from a real device operation. A good strategy to define the MESH is presented at [7] where the author suggests the creation of a MESH divided on regions with higher and lower concentration of simulation points and with the refinement of the points on areas on which the simulations are more important. In this work these regions would be the active regions and channel.

With the data extracted from [3] and [7] the device where constructed. After simulations the doping profiles and dimensions where calibrated to achieve the desired behavior and electrical characteristics. In figure 2 the developed model.

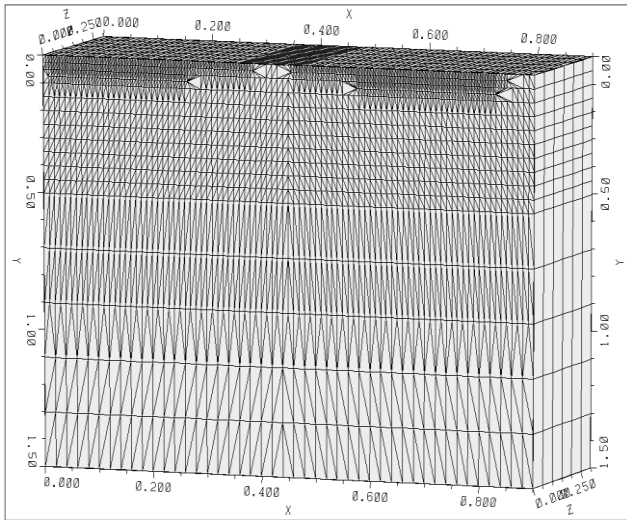


Fig. 2 - Developed NMOS 90nm device

Notice the y axis at figure 2 that from  $0.0$  to  $0.5\mu m$  the MESH has more points that from  $0.5$  to  $1.5\mu m$ . Over active regions and channel the MESH is refined to receive more simulation points. This kind of refinement is done during simulations to achieve the desired accuracy.

In table 1 the dimensions of the LDD, SSR, active regions, gate and oxide. The doping profile is also presented.

Region	Width (x)	Width (y)	Width (z)	Doping
LDD	115 nm	30 nm	240 nm	n-type. Peak: $1e19$
Source\Drain	240 nm	60 nm	240 nm	n-type. Peak: $1e20$
SSR	90 nm	5 nm	240 nm	n-type. Peak: $1.5e18$
Gate	136 nm	300 nm	240 nm	n-type. Peak: $2e20$
Oxide	136 nm	1.4 nm	240 nm	None
Substrate	0.9	1.5	0.3 $\mu m$	p-type. Peak: $5.5e18$

Table 1: Dimensions and doping profiles

The doping has Gaussian distribution. The difference of doping between Substrate and SSR is used to control the threshold of the device. Using an uniform substrate doping the threshold of the device was too high almost near  $VDD$  ( $1.2$  V for this device) and the SSR was used to reduce its value. The oxide was not adjusted to control the threshold voltage and this value is the same that [7] had been used to  $90$  nm high performance devices.

### 4. SIMULATION RESULTS

To validate the NMOS transistor, simulations were conducted to analyze the behavior of the device when a bias is applied at terminals (substrate, source, gate, drain). Over the simulations in figure 3 and 4 the substrate and source where grounded ( $V_s=V_b=0V$ ). At figure 3 the  $V_{ds}$  is fixed on  $1.2$  V and a bias is applied on the gate terminal.

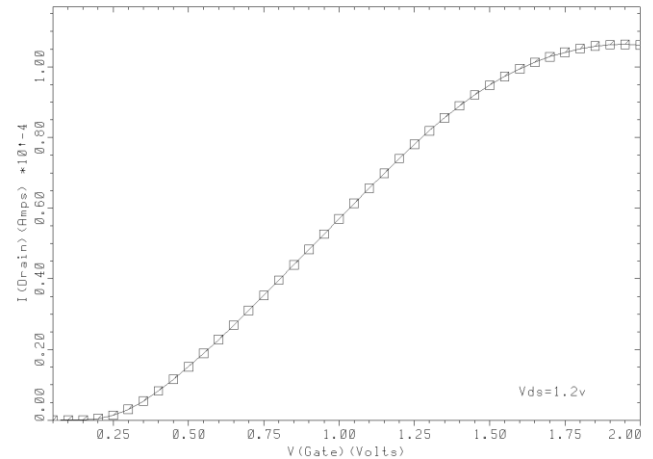


Fig. 3 - Ids vs Vgs

To validate the agreement of the model with electrical parameters of a  $90$  nm device, simulations where conducted using a PTM available in reference [8]. The threshold voltage of the PTM model was about  $V_t=0.29$  V. The document of design rules from ST  $90$ nm [9] indicates a  $V_t=0.34$  V for high speed devices of that technology. The threshold voltage of the developed model was obtained by MOS parameter extraction command of TCAD and is about  $V_t=0.36$  V. The sub-

threshold slope of the device was found to be 69.6 mV/decade.

The range of the measure sub-threshold slope also fits with the measurements in reference [10]. At the work mentioned before the author makes an extensive analysis of different parameters (oxide, channel length) and their effect over the sub-threshold.

The scale of the simulation ( $I_{ds}$  vs  $V_{ds}$ ) of the PTM model and results from the reference [7] also fits with the results of the developed device. In figure 4 the  $V_{gs}$  is fixed on 1.2 V and the drain bias is varied.

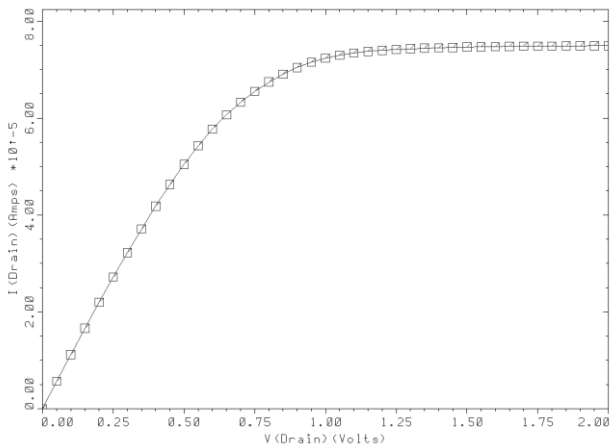


Fig. 4 -  $I_{ds}$  vs  $V_{ds}$  simulation

With these figures the main behavior of the transistor is verified. The last simulations were conducted using Newton and Incomplete Cholesky Conjugate Gradients (ICCG) numerical methods.

As the device has a small oxide (1.4 nm), the effects of the tunnel mechanism were also evaluated.

In Figure 5 the direct tunneling analysis for a  $V_{ds}=0$  V.

#### Tunneling Analysis over Device

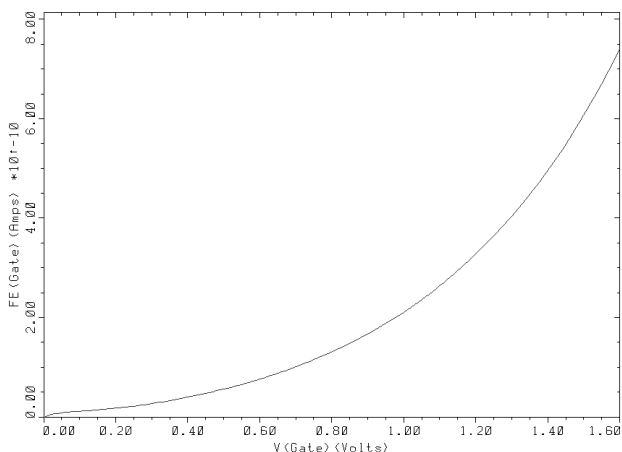


Fig 5 – Direct Tunneling  $V_{ds}=0$  V

At temperature with 300 K and  $V_{ds}=0V$  the current at  $V_g=1.2$  V is about 0.32nA. The  $FE(Gate)$  is the direct tunneling current function used by Davinci. The direct tunneling current was also evaluated for different

drain bias conditions. At the next figure the analysis for different bias.

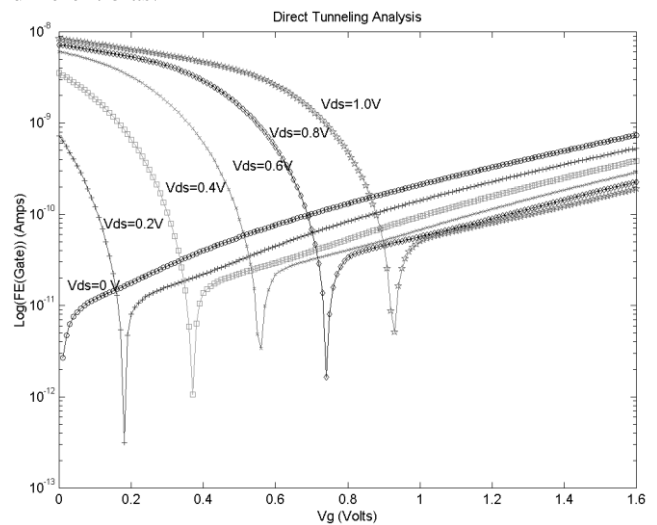


Figure 6: Direct Tunneling Analysis

The figure 6 is in logarithmic scale and shows the current flowing through the channel to the gate and gate to channel. At the left part of the figure from  $V_{ds}=0.2$  V to  $V_{ds}=1.0$  V is possible to notice that the current start to drawn until a certain point near the  $V_g$  with a value near the used  $V_{ds}$ . At this point the current is negative and is flowing from channel to the gate. After this point the current becomes positive what mean that the current is flowing through the gate to the channel.

In reference [11] the author exposed the main components of the gate tunnel current. The inversion of the current signal in the figure 6 is explained by the increase of the gate current. When  $V_{ds}$  bias is greater them  $V_{gs}$  the current is passed from the substrate (channel) to the gate, this behavior is changed when the bias of  $V_{gs}$  reach  $V_{ds}$  and the current start to take the inverse path.

These simulations were solved using the numerical integration of the Gundlach Tunneling Coefficient. The direct tunneling analysis combines both direct tunneling regime and the Fowler-Nordheim regime.

In Figure 7 the bias of regions of the device during operation ( $V_{gs}=1.2$  V).

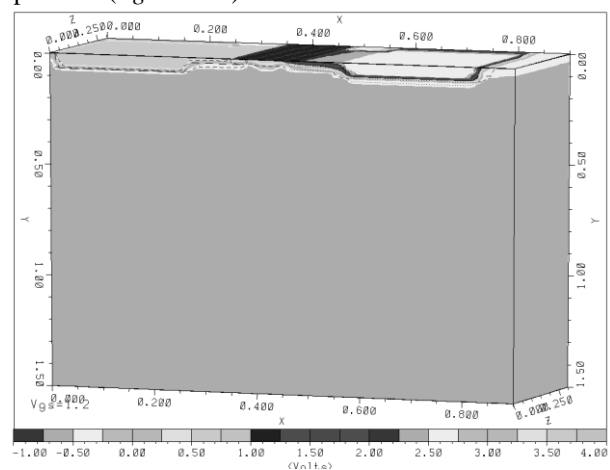


Fig. 7 - Device operation at  $V_{gs}=1.2$  V.

The Figure 7 shows the *NMOS* transistor during operation, its is possible to notice the difference between the voltage of the substrate and source, which is a body effect that changes the threshold of the transistor.

## 5. CONCLUSIONS

This paper presents the modeling of a *NMOS* 90nm device in Davinci tool from Synopsys. Results comparing the device with PTM simulations and values extracted from [7] and ST 90 nm shows a good agreement with the model.

The threshold of the device was pretty near the  $V_t$  of ST 90 nm High Speed device and the sub-threshold slope of the device was measured and is equal to  $69.6mV/dec$ .

The direct tunneling current was evaluated showing the behavior of the device to the oxide of  $1.5\text{ nm}$ . The measured tunneling current was about  $0.32nA$  to a  $V_{ds}=0V$  and  $V_g=1.2\text{ V}$ .

## 10. REFERENCES

- [1] TSIVIDIS, Y. **Operation and Modeling of The MOS Transistor**. Second Edition. New York: Oxford University, 1999, 620 p.
- [2] SYNOPSIS. **Taurus Medicis Davinci User Guide**. Version Y-2006.06 June 2006.
- [3] MIT. **Well-Tempered Bulk-Si NMOSFET Device**. Microsystems Technology Laboratory, Massachusetts institute of technology (MIT). <Available at: <http://www-mtl.mit.edu/researchgroups/Well/>>. 2008.
- [4] HU. H. et al., IEEE TED-42(4), p. 669, 1995
- [5] SRINIVASAN, R.; BHAT, N. **Impact of Channel Engineering on Unity Gain Frequency and Noise-Figure in 90nm NMOS Transistors for RF Applications**. International Conference on VLSI Design. 2005.
- [6] TIAN, H. HULFACHOR, R.B. et al. **An Evaluation of Super-Steep-Retrograde Channel Doping for Deep-Submicron MOSFET Applications**. IEEE TRANSACTIONS ON ELECTRON DEVICES, VOL. 41, NO.10. OCTOBER 1994.
- [7] DASGUPTA, S. **Trends in Single Event Pulse Width and Pulse Shapes in Deep Submicron CMOS**. Thesis from the Faculty of the Graduate School of Vanderbilt University. Electrical Engineering. Vanderbilt University. Nashville, Tennessee. USA. 2007.
- [8] ASU. **Predictive Technology Model . Nanoscale Integration and Modeling** Group. Arizona State University (ASU). <Available at: <http://www.eas.asu.edu/~ptm/>>. 2008.
- [9] STMicroelectronics. **HCMOS9\_GP Design Rules Manual 013 MICRON CMOS PROCESS**. Date 11-Apr-02.
- [10] HANSON, S.; SEOK, M.; SYLVESTE, D.; BLAAUW, D. **Nanometer Device Scaling in Subthreshold Circuits**. DAC 2007, San Diego, California. USA.
- [11] MAJKUSIAK, B. **Gate Tunnel Current in MOS Transistors**. IEEE TRANSACTIONS ON ELECTRON DEVICES. Vol. 37, No. 4. April. 1990.